Artificial Intelligence Research and Development
T. Alsinet et al. (Eds.)

doi:10.3233/FAIA240422

Open Source Cardiac Digital Twinning of Human Ventricular Repolarisation from 12-Lead ECG and MRI

Julia Camps[a,1,*], Zhinuo Jenny Wang[a,*], Ruben Doste[a], Lucas Arantes Berg[a], Maxx Holmes[a], Brodie Lawson[b], Jakub Tomek[c], Kevin Burrage[b], Alfonso Bueno-Orovio[a], Blanca Rodriguez[a]
[a] *Department of Computer Science, University of Oxford, UK*
[b] *Department of Physiology, Anatomy & Genetics, University of Oxford, UK*
[c] *Queensland University of Technology, Australia*
ORCIDs: Julia Camps https://orcid.org/0000-0002-6491-2565,
Zhinuo Jenny Wang https://orcid.org/0000-0001-5325-909X,
Ruben Doste https://orcid.org/0000-0003-4187-4970,
Lucas Arantes Berg https://orcid.org/0000-0002-8777-0125

Abstract. Cardiac digital twins represent the required functional mechanisms of patient hearts to evaluate therapies and inform clinical decision-making virtually. A scalable generation of cardiac digital twins can enable virtual clinical trials on virtual cohorts to fast-track therapy development. Here, we present an open-source digital twinning framework for personalising electrophysiological function based on routinely acquired magnetic resonance imaging (MRI) data and the standard 12-lead electrocardiogram (ECG). We extended a Bayesian-based inference framework to infer electrical repolarisation characteristics. Fast simulations are conducted with a decoupled reaction-Eikonal model, including the Purkinje network and biophysically-detailed subcellular ionic current dynamics. Parameter uncertainty is represented by inferring a population of ventricular models rather than a single one, which means that parameter uncertainty can be propagated to virtual therapy evaluations. The framework is demonstrated in a healthy female subject, where our inferred reaction-Eikonal models reproduced the patient's ECG with a Pearson's correlation coefficient of 0.93. The methodologies for cardiac digital twinning presented here are a step towards personalised virtual therapy testing. The tools developed for this study are open-source, ensuring accessibility, inclusivity, and reproducibility, this is available on GitHub.

Keywords. Digital twin; Eikonal model; Magnetic resonance imaging; Electrocardiogram; Uncertainty quantification; Bayesian inference; Open source

1. Introduction

A cardiac digital twin is a suite of tools that continuously and coherently integrate patient data to produce virtual hearts to help realise the vision of precision medicine in

[1] Corresponding Author: Julia Camps, julcamps@gmail.com

[*] Julia Camps and Zhinuo Jenny Wang made equal contributions to this work.

cardiology (1). For such cardiac digital twin technologies to be useful for therapy development, computational modelling choices should ensure that the critical therapy targets are represented sufficiently, that only non-invasive data is required for building the digital twins (2), and that their parameter uncertainty is propagated when informing clinical decision-making. Here, we present a cardiac digital twin generation framework developed with these goals, using routinely acquired magnetic resonance imaging (MRI) data and 12-lead electrocardiograms (ECG).

The ECG encodes information about activation and repolarisation properties: the QRS complex of the ECG reflects the activation pattern. At the same time, the ECG ST segment and T wave comprise information on spatial heterogeneities in repolarisation and action potential duration (APD) (3,4). Repolarisation heterogeneities are underpinned by a complex interplay of subcellular ionic current dynamics (3,4), which are altered by antiarrhythmic drugs, such as Dofetilide. Therefore, phenomenological models that do not explicitly describe these ionic currents are of limited relevance in the context of virtual drug evaluations (5). However, the high computational cost of simulating electrotonic coupling with human-based ionic current dynamics using either the gold standard reaction-diffusion equations (6) limits the scalability of the digital twin generation framework. Therefore, this paper presents a strategy that leverages the benefits of both phenomenological and biophysically detailed models to enable scalable and relevant cardiac digital twins towards large-scale therapy evaluation.

2. Methods

As an overview (Figure 1), this study extends our previous framework (1,7,8) to automatically infer the activation and repolarisation properties of a biophysically detailed cardiac electrophysiological model from MRI and 12-lead ECG (Figure 1). The framework is demonstrated in a healthy female subject whose biventricular cardiac geometry was extracted from MRI (9). The tetrahedral mesh had a resolution of 1.5 mm edge length. The subject's clinical 12-lead ECG recordings were preprocessed as in (1). The fibre, sheet, and sheet-normal vector fields were obtained as in (10).

Fast inference was enabled by developing a decoupled reaction-Eikonal model that incorporated biophysically detailed electrophysiology (11) stimulated with a realistic diffusion-like current (12). While the activation properties were previously inferred using the QRS complex in (1), we focus on inferring smooth spatial variations in APDs from the ECG ST segment and T wave signals (Figure 1).

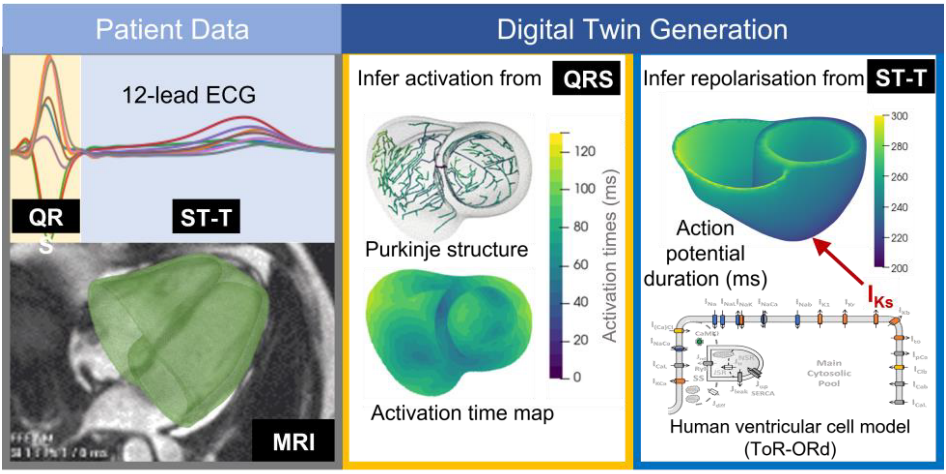

Figure 1. Overview of our cardiac digital twin personalisation framework. The framework infers the conduction speeds and the Purkinje-informed locations of earliest endocardial activations from matching QRS simulations to the clinical ECG. Then, the framework infers the APD spatial heterogeneity with the slow delayed rectifier potassium current (IKs) by matching simulations to the clinical ECG ST segment and T wave signals.

2.1. Action potential duration gradients model

Spatial heterogeneity in APD, defined at 90% of repolarisation (APD90 or just APD for this study), was represented by a weighted linear sum of four ventricular coordinates (5) calculated using the position of a mesh node in three-dimensional space, $\boldsymbol{x}$. These coordinates are the apex-to-base coordinate $ab(\boldsymbol{x})$ as in (13), the transmural coordinate $tm(\boldsymbol{x})$ as in (14), and the transventricular coordinate (left-to-right ventricle) $tv(\boldsymbol{x})$, and the posterior-to-anterior $pa(\boldsymbol{x})$ coordinate as in (15). These coordinates are used to define a spatially varying APD field (Figure 2) that ranges between a specified minimum (APD_{min}) and maximum (APD_{max}) value, as follows

$$\mathrm{APD}(\boldsymbol{x}) = \left(\frac{q(\boldsymbol{x})-q(\boldsymbol{x})_{min}}{q(\boldsymbol{x})_{max}-q(\boldsymbol{x})_{min}}\right)(APD_{max} - APD_{min}) + APD_{min}\,, \tag{1}$$

$$q(\boldsymbol{x}) = g_{ab}ab(\boldsymbol{x}) + g_{tm}tm(\boldsymbol{x}) + g_{pa}pa(\boldsymbol{x}) + g_{tv}tv(\boldsymbol{x})\,, \tag{2}$$

The weighting parameters g_{ab}, g_{tm}, g_{pa}, and g_{tv} in Eq. (2) control the relative magnitude of the APD gradient in their respective coordinate directions.

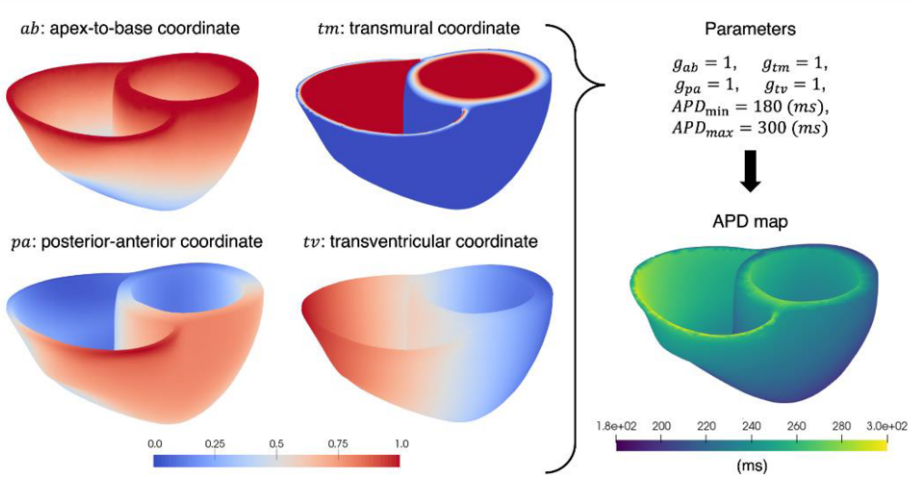

Figure 2. Biventricular coordinates were used to produce a representative APD map, which is generated using a linear combination of gradient weights (g_{ab}, g_{tm}, g_{pa}, and g_{tv}) along these coordinates with a specified APD range $[APD_{min}, APD_{max}]$.

2.2. Decoupled Reaction-Eikonal model of human cardiac electrophysiology

One of the main hurdles for generating cardiac digital twins is the high computational cost of simulating mechanistic models of cardiac electrophysiology, such as monodomain simulations, that enable virtual therapy evaluation. To overcome this challenge, we implement a decoupled dictionary-based reaction-Eikonal model

$$\begin{cases} U(\boldsymbol{x}, t) = U_{rest} + H\big(t - t_a(\boldsymbol{x})\big)K_{A,\tau} \\ A = [APD],\ \tau = \min([t - t_a(\boldsymbol{x})], t_{max}) \end{cases}, \tag{3}$$

where $U(\boldsymbol{x}, t)$ is the membrane potential transient field, which varies spatially over mesh nodes $\boldsymbol{x}$ and temporally over t, U_{rest} is the resting membrane potential before the action potential's upstroke, H is the Heaviside function, and square brackets indicate rounding to integer values. The time of electrical activation, $t_a(\boldsymbol{x})$, is given by the Eikonal model

$$\begin{cases} \sqrt{\nabla t_a^T(\boldsymbol{x})\boldsymbol{V}\nabla t_a(\boldsymbol{x})} = 1 \qquad in\ \Omega_{\boldsymbol{x}} \\ t_a(\boldsymbol{x}) = t_i \qquad for\ \boldsymbol{x} = \boldsymbol{y}_i, where\ i = 1..n \end{cases}, \tag{4}$$

where $\boldsymbol{V}$ is the conduction velocity tensor (prescribing orthotropic conduction in the fibre, sheet, and normal directions), and t_i is the activation times of the n earliest activation root nodes located at $\boldsymbol{y}_i$. In Eq. (3), K is a precomputed dictionary (i.e., lookup table) that uniquely maps integer values of APD ($A = [APD]$) and time within the course of the action potential (τ) to a corresponding membrane potential U:

$$K : A, \tau \rightarrow U\ , \tag{5}$$

The action potentials $U(\tau)$ were computed by solving the ordinary differential equation

$$\frac{dU}{d\tau} = I_{stim} + I_{ion}\,, \tag{6}$$

where I_{ion} is the sum of ionic currents in a human-based model of ventricular cardiomyocyte electrophysiology (ToR-ORd) (11), which we get using dictionary K, and I_{stim} is a stimulus current derived to mimic a diffusion current as in (12).

The dictionary K was precomputed by simulating a population of cell models (16) by uniformly sampling I_{Ks} conductance (G_{Ks}) varying between 1/50 to 50-fold its baseline value (17,18).

2.3. Electrocardiogram simulation

Standard 12-lead ECGs were simulated from the decoupled reaction-Eikonal membrane potential simulations $U(\boldsymbol{x}, t)$ using the pseudo-ECG method (19,8). The simulated ECGs are normalised to the R-progression of the clinical data (1). Body surface potentials, Φ, were calculated at the electrode locations ($\boldsymbol{x}'$) using:

$$\Phi(\boldsymbol{x}') = \sum_{j=1}^{N_{src}} -\boldsymbol{D}_j (\nabla U)_j \left[\nabla \frac{b_j}{r_j}\right], \tag{7}$$

where $(\nabla U)_j$ is the spatial gradient of the membrane potential over the j th tetrahedral element, $\boldsymbol{D}_j$ is the diffusivity tensor at the jth element, b_j is the normalised volume scaling factor for the j th element, r_j is the Euclidean distance from the centroid of the j-th element to the electrode location($\boldsymbol{x}'$), and N_{src} is the total number of tetrahedral source elements.

2.4. Inference of repolarisation gradients to match ST and T wave ECG signals

After inferring the biventricular electrical activation pattern is inferred from the 12-lead QRS ECG segment using (1), the SMC-ABC algorithm (8) was adapted to infer the APD ranges and spatial gradients: g_{ab}, g_{tm}, g_{pa}, g_{tv}, APD_{min}, APD_{max}, in Eqs. (1) and (2).

A starting population of size 256 was created using Latin Hypercube Sampling of the parameters, and the objective function (ϵ) was evaluated per sample in the population as

$$\epsilon = 100 \times \frac{1}{L}\sum_{i=0}^{L}(1 - PCC_i)^2 + 2 \times \frac{\frac{1}{L}\sum_{i}^{L} RMSE_i}{\max(|ECG_{clinical}|)}\,, \tag{8}$$

where PCC_i and $RMSE_i$ are the Pearson's correlation coefficient (PCC), and root mean squared error (RMSE) for the ECG lead i between the simulated and clinical ECG signals, and $\max(|ECG_{clinical}|)$ is the maximum amplitude across all leads of the normalised clinical ECG data. All ECGs were normalised, so these errors have no units.

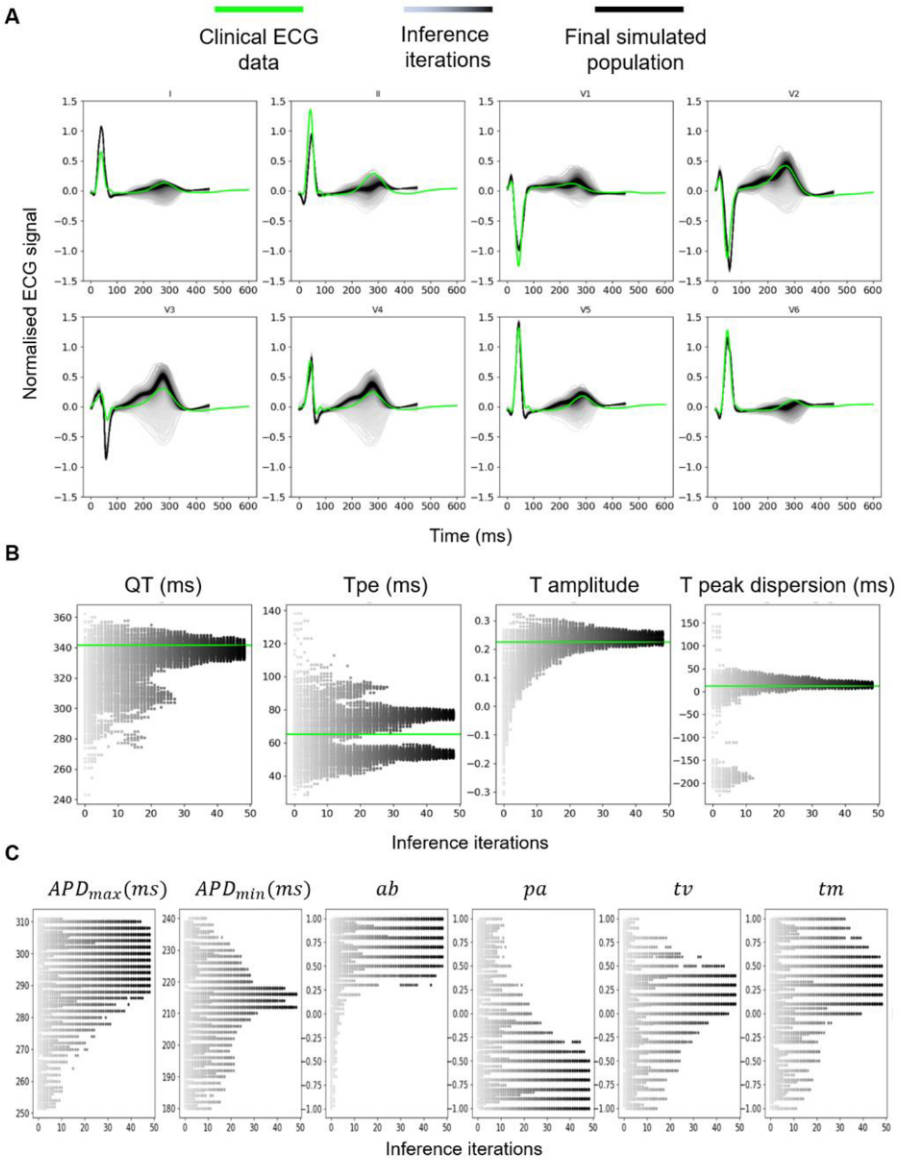

Figure 3. Inference iterations effectively explore T wave biomarker space. The evolution of the inferred population throughout the inference process is shown in greyscale with increased saturation, indicating the iteration number from 1 to 50. The final inferred results (iteration 50) are shown in black. A) ECG simulation evolution throughout the inference process. B) Simulated QT interval, T-peak to T-end interval (Tpe), average T wave amplitude, dispersion of T peak timing between V3 and V5 evolution (greyscale), and clinical values (lime horizontal line). C) Evolution of the parameter space.

3. Results

The inferred population was able to match both QRS and T wave morphologies in the clinical data (Figure 3B), achieving a Pearson's correlation coefficient (PCC) of 0.93 ± 0.0003 and a discrepancy Eq. (8) of 0.74. The inference process was terminated by the uniqueness threshold rather than the discrepancy cut-off, which had been set to 0.5, meaning that the final population had less than 50% uniqueness in the parameter sets (8).

The inference process explored a wide range of T wave biomarker values over 50 iterations (grayscale gradients in Figure 3) before arriving at the final population. The mean and standard deviation of the inferred parameters in the final population were $APD_{min} = 216 \pm 0\, ms$, $APD_{max} = 298 \pm 4.8\, ms$, $g_{ab} = 0.86 \pm 0.12$, $g_{pa} = -0.79 \pm 0.14$, $g_{tv} = 0.22 \pm 0.09$, $g_{tm} = 0.21 \pm 0.14$. Interestingly, the T-peak to T-end (Tpe) biomarker converged into two cluster values. In contrast, all other biomarkers seemed to have a single cluster of values in the final population.

We compared the performance of our decoupled reaction-Eikonal model to other electrophysiology propagation models in the literature (Table 1). We demonstrated a similar computational cost to the reaction-Eikonal without diffusion (20).

Table 1. Computation times for different electrophysiology propagation models in the literature using non-high-performance-computing resources on biventricular meshes at different discretisation (edge length) resolutions. Our decoupled reaction-Eikonal's computation time (last row) was computed by averaging the cost of 128 simulations.

Model	Anatomy setup	Computer specifications	Simulation cost of 450 ms
Monodomain (21) with ECG calculation	Mesh at 0.5 mm	Eight cores and 1 GPU (NVIDIA A100)	12 min
Reaction-diffusion-Eikonal (RE+) (20) without ECG	Mesh at 1 mm	16 cores	197 sec (5)
Reaction-Eikonal (RE-) (20) without the ECG	Mesh at 1 mm	16 cores	8 sec (5)
Our decoupled reaction-Eikonal with ECG	Mesh at 1.5 mm	32 cores	4 sec

4. Discussion

We extend our previous open-source cardiac digital twin generation framework (8,1) to calibrate the human ventricular repolarisation parameters from clinical 12-lead ECG and MRI. We demonstrate its application to augment clinical data from one control subject, where we matched the clinical data with a PCC of 0.93 ± 0.0003 between the simulated and clinical ECG recordings. The key novelty is the personalisation of repolarisation heterogeneities using a fast (Table 1) dictionary-based decoupled reaction-Eikonal model.

While calibration of repolarisation characteristics using the 12-lead ECG has been achieved in a previous study (5), their ventricular model relied on phenomenological models of cellular electrophysiology. The lack of biophysical ionic detail and human

relevance presents a significant hurdle for such methods for drug therapy testing and disease mechanism explorations (22). In this study, we provide a novel strategy incorporating a state-of-the-art human-based ventricular electrophysiological model.

Our inference method matched the final inferred population's ECG ST segment and T wave. Rather than selecting a single best match, the SMC-ABC method allows us to recover a population with similarly suitable clinical data matches (Figure 3). Propagating this uncertainty is critical for realising virtual clinical trials (23) using cardiac digital twins (8,1,18).

While we demonstrated the digital twinning results on a female subject, additional use cases in different subjects have been previously reported (8,1,18), suggesting that these methods can robustly generalise to new subjects (male and female).

The Cardiac Digital Twinning framework is open-source and can be downloaded with examples from https://github.com/juliacamps/Cardiac-Digital-Twin.

Acknowledgements

This work was funded by an Engineering and Physical Sciences Research Council doctoral award to Julia Camps, a Wellcome Trust Fellowship in Basic Biomedical Sciences to Blanca Rodriguez (214290/Z/18/Z), the PRACE ICEI project icp013 and icp019, the EPSRC project CompBioMed X (EP/X019446/1) and the CompBioMed 2 Centre of Excellence in Computational Biomedicine (European Commission Horizon 2020 research and innovation programme, grant agreements No. 675451 and No. 823712, respectively), the Australian Research Council Centre of Excellence for Mathematical and Statistical Frontiers (CE140100049), an Australian Research Council Discovery Project (DP200102101), by the Queensland University of Technology (QUT) through the Centre for Data Science. This study used high-performance-computing resources from the Piz Daint at the Swiss National Supercomputing Centre, Switzerland, the JURECA machine at the Juelich Supercomputing Centre, Germany, the Polaris supercomputer at the Argonne Leadership Computing Facility (ALCF), Argonne National Laboratory, United States of America. The U.S. Department of Energy's (DOE) Innovative and Novel Computational Impact on Theory and Experiment (INCITE) Program awarded access to Polaris. The ACLF is supported by the Office of Science of the U.S. DOE under Contract No. DE-AC02-06CH11357.

References

1. Camps J, Berg LA, Wang ZJ, Sebastian R, Riebel LL, Doste R, et al. Digital twinning of the human ventricular activation sequence to Clinical 12-lead ECGs and magnetic resonance imaging using realistic Purkinje networks for in silico clinical trials. Medical Image Analysis. 2024 May 1;94:103108.

2. Li L, Camps J, Rodriguez B, Grau V. Solving the Inverse Problem of Electrocardiography for Cardiac Digital Twins: A Survey . arXiv; 2024.

3. Szentadrassy N, Banyasz T, Biro T, Szabo G, Toth BI, Magyar J, et al. Apico–basal inhomogeneity in distribution of ion channels in canine and human ventricular myocardium. Cardiovascular Research. 2005 Mar 1;65(4):851–60.

4. Opthof T, Remme CA, Jorge E, Noriega F, Wiegerinck RF, Tasiam A, et al. Cardiac activation–repolarization patterns and ion channel expression mapping in intact isolated normal human hearts. Heart Rhythm. 2017 Feb 1;14(2):265–72.

5. Gillette K, Gsell MAF, Prassl AJ, Karabelas E, Reiter U, Reiter G, et al. A Framework for the generation of digital twins of cardiac electrophysiology from clinical 12-leads ECGs. Medical Image Analysis. 2021 Jul 1;71:102080.

6. Potse M, Dube B, Richer J, Vinet A, Gulrajani RM. A Comparison of Monodomain and Bidomain Reaction-Diffusion Models for Action Potential Propagation in the Human Heart. IEEE Transactions on Biomedical Engineering. 2006 Dec;53(12):2425–35.

7. Banerjee A, Camps J, Zacur E, Andrews CM, Rudy Y, Choudhury RP, et al. A completely automated pipeline for 3D reconstruction of human heart from 2D cine magnetic resonance slices. Philosophical Transactions of the Royal Society A: Mathematical, Physical and Engineering Sciences. 2021 Dec 13;379(2212):20200257.

8. Camps J, Lawson B, Drovandi C, Minchole A, Wang ZJ, Grau V, et al. Inference of ventricular activation properties from non-invasive electrocardiography. Medical Image Analysis. 2021 Oct 1;73:102143.

9. Mincholé A, Zacur E, Ariga R, Grau V, Rodriguez B. MRI-Based Computational Torso/Biventricular Multiscale Models to Investigate the Impact of Anatomical Variability on the ECG QRS Complex. Front Physiol . 2019;10.

10. Levrero-Florencio F, Margara F, Zacur E, Bueno-Orovio A, Wang ZJ, Santiago A, et al. Sensitivity analysis of a strongly-coupled human-based electromechanical cardiac model: Effect of mechanical parameters on physiologically relevant biomarkers. Computer Methods in Applied Mechanics and Engineering. 2020 Apr 1;361:112762.

11. Tomek J, Bueno-Orovio A, Passini E, Zhou X, Minchole A, Britton O, et al. Development, calibration, and validation of a novel human ventricular myocyte model in health, disease, and drug block. Faraldo-Gómez JD, Barkai N, Hund T, Maleckar M, editors. eLife. 2019 Dec 23;8:e48890.

12. Gassa N, Zemzemi N, Corrado C, Coudière Y. Spiral Waves Generation Using an Eikonal-Reaction Cardiac Electrophysiology Model. In: Ennis DB, Perotti LE, Wang VY, editors. Functional Imaging and Modeling of the Heart. Cham: Springer International Publishing; 2021. p. 523–30. (LNCS; vol. 12738).

13. Schuler S, Pilia N, Potyagaylo D, Loewe A. Cobiveco: Consistent biventricular coordinates for precise and intuitive description of position in the heart – with MATLAB implementation. Medical Image Analysis. 2021 Dec 1;74:102247.

14. Bayer J, Prassl AJ, Pashaei A, Gomez JF, Frontera A, Neic A, et al. Universal ventricular coordinates: A generic framework for describing position within the heart and transferring data. Medical Image Analysis. 2018 Apr 1;45:83–93.

15. Doste R, Soto-Iglesias D, Bernardino G, Alcaine A, Sebastian R, Giffard-Roisin S, et al. A rule-based method to model myocardial fiber orientation in cardiac biventricular geometries with outflow tracts. International Journal for Numerical Methods in Biomedical Engineering. 2019;35(4):e3185.

16. Passini E, Trovato C, Morissette P, Sannajust F, Bueno-Orovio A, Rodriguez B. Drug-induced shortening of the electromechanical window is an effective biomarker for in silico prediction of clinical risk of arrhythmias. British Journal of Pharmacology. 2019;176(19):3819–33.

17. Doste R, Coppini R, Bueno-Orovio A. Remodelling of potassium currents underlies arrhythmic action potential prolongation under beta-adrenergic stimulation in hypertrophic cardiomyopathy. Journal of Molecular and Cellular Cardiology. 2022 Nov 1;172:120–31.

18. Camps J, Wang ZJ, Doste R, Holmes M, Lawson B, Tomek J, et al. Cardiac Digital Twin Pipeline for Virtual Therapy Evaluation . arXiv; 2024.

19. Gima K, Rudy Y. Ionic Current Basis of Electrocardiographic Waveforms: A Model Study. Circulation Research. 2002 May 3;90(8):889–96.

20. Neic A, Campos FO, Prassl AJ, Niederer SA, Bishop MJ, Vigmond EJ, et al. Efficient computation of electrograms and ECGs in human whole heart simulations using a reaction-eikonal model. J Comput Phys. 2017 Oct 1;346:191–211.

21. Sachetto Oliveira R, Martins Rocha B, Burgarelli D, Meira Jr. W, Constantinides C, Weber dos Santos R. Performance evaluation of GPU parallelization, space-time adaptive algorithms, and their combination for simulating cardiac electrophysiology. International Journal for Numerical Methods in Biomedical Engineering. 2018;34(2):e2913.

22. Zhou X, Wang ZJ, Camps J, Tomek J, Santiago A, Quintanas A, et al. Clinical phenotypes in acute and chronic infarction explained through human ventricular electromechanical modelling and simulations. eLife . 2024 Feb 23;13.

23. Musuamba FT, Skottheim Rusten I, Lesage R, Russo G, Bursi R, Emili L, et al. Scientific and regulatory evaluation of mechanistic in silico drug and disease models in drug development: Building model credibility. CPT: Pharmacometrics & Systems Pharmacology. 2021;10(8):804–25.